Lasers Med Sci (2013) 28:717–724
DOI 10.1007/s10103-012-1122-3

ORIGINAL ARTICLE

Effect of 635 nm irradiation on high glucose-boosted inflammatory responses in LPS-induced MC3T3-E1 cells

HyukIl Kwon · WonBong Lim · JiSun Kim · SangMi Jeon · SangWoo Kim · Sandeep Karna · HyunRok Cha · OkJoon Kim · HongRan Choi

Received: 11 August 2011 / Accepted: 7 May 2012 / Published online: 15 June 2012

Abstract Hyperglycemia occurs in patients with poorly controlled diabetes mellitus and contributes to bone resorption and increased susceptibility to bacterial infections. Hyperglycemia can incite low-grade inflammation that can contribute to the resorption of bone, especially the periodontal bone. The increased susceptibility to periodontal infections can contribute to bone resorption through the activation of osteoclasts. In this study, the osteoblastic, clonal cell line, MC3T3-E1, was used in an in vitro model of hyperglycemia and lipopolysaccharide-induced reactive oxygen species generation to determine the potential anti-inflammatory effect of 635 nm light-emitting diode (LED) irradiation or whether 635 nm LED irradiation can be a potential anti-inflammatory treatment. LED irradiation of MC3T3-E1 cells stimulated with lipopolysaccharide in a high glucose-containing medium decreased the level of cyclooxygenase gene and protein expression and reduced the level of prostaglandin E2 expression by decreasing the amount of reactive oxygen species generation. LED irradiation also inhibited the osteoclastogenesis in MC3T3-E1 cells by regulating the receptor activator of nuclear factor kappa-B ligand and osteoprotegerin. These findings reveal the mechanisms which are important in the pathogenesis of diabetic periodontitis and highlight the beneficial effects of 635 nm LED irradiation in reducing the adverse effects of diabetic periodontitis.

Keywords Diabetes mellitus · Glucose · Lipopolysaccharide · Periodontitis · ROS

Introduction

Clinical studies have established that periodontitis is more prevalent and severe in patients with either type 1 or type 2 diabetes than in non-diabetic patients [1]. Diabetic periodontitis is a chronic inflammatory disease of the supporting tissues of the teeth, which is generally believed to be caused by Gram-negative bacteria, and is characterized by gingival inflammation and bone resorption [2]. Hyperglycemia, a major metabolic disorder in both type 1 and type 2 diabetes, can induce diabetic periodontitis via the impaired host defense against bacterial infections and the increased susceptibility to infection [1, 3–6].

Previous studies showed that multiple mechanisms are involved in the pathogenesis and progression of diabetes-associated periodontal disease [1]. Diabetic periodontitis is generally induced by bacterial pathogens such as *Porphyromonas gingivalis*, which is a Gram-negative bacterium that releases lipopolysaccharide (LPS). LPS, a Gram-negative bacteria-derived product, has long been recognized as a potent stimulator of the inflammatory pathway in osteoblasts [7]. LPS initiates a local host response in bone tissues that involves the recruitment of inflammatory cells, such as prostanoids and cytokines, which stimulate prostaglandin E_2 (PGE_2) production in osteoblasts through cyclooxygenase (COX) overexpression. COX exists in two isoforms: a constitutively expressed COX-1 and an inducible COX-2. COX

These first two authors, HyukIl Kwon and WonBong Lim, contributed equally to this work.

H. Kwon · W. Lim · J. Kim · S. Jeon · S. Kim · S. Karna · O. Kim · H. Choi (✉)
Department of Oral Pathology, School of Dentistry, Dental Science Research Institute, Chonnam National University, Bug-Gu, Gwangju 500-757, South Korea
e-mail: hongran@chonnam.ac.kr

H. Cha
Korea Institute of Industrial Technology, Cheonan, South Korea

is a key enzyme for PGE_2 production, which can mediate the inflammatory response and induce bone resorption by stimulating osteoclast differentiation [8, 9]. Some studies reported that LPS stimulates receptor activator of nuclear factor kappa-B ligand (RANKL) expression in osteoblasts and suppresses osteoprotegerin (OPG) expression by enhancing PGE_2 production [8]. The formation and maintenance of bone tissues are regulated by bone-forming osteoblasts and bone-resorbing osteoclasts. Osteoblasts produce RANKL, which exerts its effects on the formation and function of osteoclasts by binding to its receptor, receptor activator of NF-κB (RANK), expressed on the osteoclast precursors and mature osteoclasts. RANKL also has a decoy receptor, OPG, which inhibits osteoclast formation by competing with RANK for binding RANKL [8].

In recent years, the physiological anti-inflammatory and wound healing effects of light irradiation with a specific wavelength were studied intensively in the clinical field. Previous studies suggested that irradiation with 600–1,100 nm wavelength from lasers or LED allows better penetration to the soft tissue than the other lights and plays a significant role as reactive oxygen species scavengers [10–14]. Recent studies also showed that 635 nm LED irradiation decreases the level of arachidonic acid-induced inflammation. However, little is known about the anti-inflammatory mechanism of 635 nm LED irradiation, especially in the diabetic periodontitis model [12]. This study examined the effect of 635 nm LED irradiation on the high glucose-boosted inflammatory response to LPS in osteoblasts in vitro.

Materials and methods

Cell culture and chemicals

MC3T3-E1 osteoblasts were cultured in alpha minimum essential medium (Gibco BRL, NY, USA) supplemented with 10 % heat inactivated fetal bovine serum (JBI, Daegu, Korea), 10 % antibiotic–antimycotic solution (JBI, Daegu, Korea) at 37 °C in a 5 % CO_2 humidified chamber. The dishes were divided randomly into four groups according to the chemical treatment: 5 mM of D-glucose (normal glucose), 25 mM of D-glucose (high glucose), normal glucose with highly purified LPS, and high glucose with highly purified LPS (InvivoGen, CA, USA) from *P. gingivalis*.

Light source and irradiation

A continuous-wave LED (U-JIN LED, Goyang, Korea) emitting at a wavelength of 635 nm with a manufactured power density of about 1 mW/cm^2 on the sample surface was used as the light source. The manufactured LED irradiation tool kit was built in a 5 % CO_2 humidified chamber at 37 °C (Fig. 1, Biophoton, Gwangju, Korea). The irradiation spot size that would fit onto a 9-cm petri dish was used. To examine the effect of 635 nm LED irradiation, each group was cultured with or without irradiation for 1 h.

Cell viability assay

To determine the LPS concentration, cells were cultured with various concentrations of LPS, and the group with 25 mM of D-mannitol (high mannitol) was added to exclude the effect of osmotic pressure on the cells. The assay for cell viability was based on the reduction of 3-(4,5-dimethylthiazol-2-yl)-2,5-diphenyltetrazolium bromide by mitochondrial dehydrogenase in viable cells to produce a purple formazan product indicating the level of cell respiration. The cells were seeded at 2×10^3 cells per well with 100 μl of the medium in 96-well plates and incubated with chemicals for 1 day at 37 °C. After incubation for 1 day, the medium was removed, and the cells were incubated in phosphate-buffered saline containing 30 μl of MTT at 37 °C for 3 h. The formazan product was dissolved in 50 μl of dimethyl sulfoxide (Calbiochem, USA). The optical density was measured at 570 nm using a colorimetric microplate reader (BioTek, Winooski, USA).

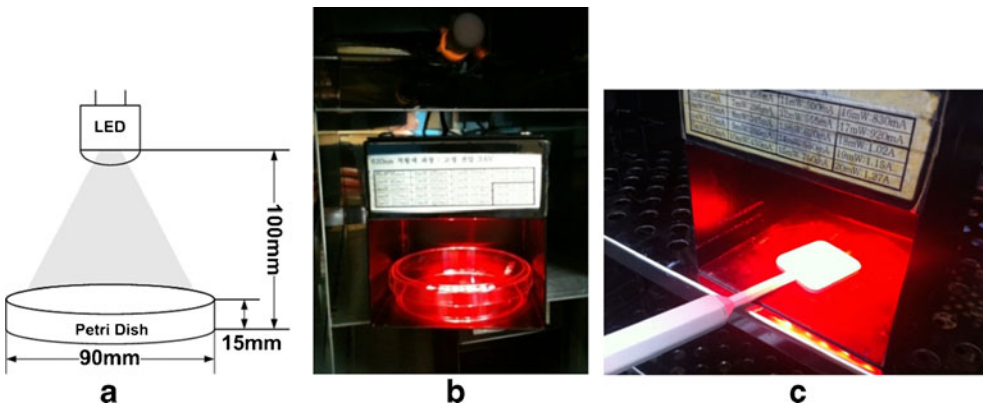

Fig. 1 Six hundred thirty-five nanometer of visible light irradiation by LED tool kit for in vitro test was built in a CO_2 humidified chamber. The figure shows the irradiation plan (**a**), irradiation in CO_2 incubator (**b**), and measurement of light power density (**c**)

Flow cytometry and laser scanning confocal microscopy analysis for the detection of reactive oxygen species (ROS) formation

At 1 day after the experiment, the ROS level was assayed using 20,70-dichlorodihydrofluorescein diacetate (Sigma, USA). 2′,7′-Dichlorofluorescein diacetate (DCF-DA) enters the cells passively, where it is deacetylated enzymatically by esterases to non-fluorescent 2,7-dihydrodichlorofluorescein (DCF-H). Oxidizing molecules, such as O_2^-, convert DCF-H to the highly fluorescent DCF. The DCF fluorescence was checked at 10 min to visualize the intracellular ROS dissociation. Cells grown on cover slips were incubated with 10 mM of DCF-DA for 20 min. Subsequently, the cells were washed with phosphate-buffered saline containing 10 mM of glucose. The DCF fluorescence intensity was monitored by confocal microscopy (Carl Zeiss, Jena, Germany) with excitation and emission wavelengths of 488 and 525 nm, respectively. After the treated cells were detached using a trypsin–EDTA solution, the ROS level was analyzed by flow cytometry (Beckman Coulter, CA, USA) using 485 nm excitation and 530 nm emission filters.

Quantitative real-time polymerase chain reaction

The total RNA was isolated from the cells using guanidinium thiocyanate–chloroform extraction (Trizol®; Gibco BRL, USA), according to the manufacturer's instructions. The complementary DNA was synthesized from the total RNA using a Maxime RT Premix kit (Intron, Korea). After 5 min at 75 °C, the reaction was carried out at 45 °C for 1 h, followed by enzyme inactivation at 95 °C for 5 min. Quantitative real-time PCR was conducted using a thermal cycler (Exicycler II™, Bioneer, CA, USA). The gene-specific primer sequences (Table 1) were designated using a gene runner NCBI and obtained from AccuOligo® (Bioneer, CA, USA). The PCR reaction mixture, consisting of a cDNA template from 1 μg/μl of the total RNA, 1 μM of each primer, and 1 μl of SYBR Green I dye (Accupower® GreenStar qPCR Premix, Bioneer, CA, USA), was amplified with a precycling activation at 95 °C for 5 min, followed by 40 cycles of denaturation at 95 °C for 20 s, and annealing at 58 °C for 40 s. Each reaction was performed in triplicate, and the levels of mRNA expression were calculated and normalized to the level of glyceraldehyde-3-phosphate dehydrogenase (GAPDH) mRNA. The data were analyzed using Exicycler II™ software (Bioneer, CA, USA).

Table 1 PCR primers used in the experiments

Target	Forward primer	Reverse primer
COX-1	5′-ACA ACT GGA GGG AGG AGT GG-3′	5′-GGG AAA CCA GAG CGA GAG AC-3′
COX-2	5′-TTC GGG AGC ACA ACA GAG TG-3′	5′-TAA CCG CTC AGG TGT TGC AC-3′
RANKL	5′-CAT GTG CCA CTG AGA ACC TTG AA-3′	5′-CAG GTC CCA GCG CAA TGT AAC-3′
OPG	5′-CAA TGG CTG GCT TGG TTT CAT AG-3′	5′-CTG AAC CAG ACA TGA CAG CTG GA-3′
GAPDH	5′-AAA TGG TGA AGG TCG GTG TG-3′	5′-TGA AGG GGT CGT TGA TGG-3′

Enzyme-linked immunosorbent assay

The amount of PGE_2, RANKL, and OPG (Quantikine®; R&D Systems, MN, USA) in the supernatants was measured using a commercially available enzyme immunoassay kit (R&D System, MN, USA) according to the manufacturer's protocol. The absorbance of PGE_2, RANKL, and OPG was measured at 450 nm using a colorimetric microplate reader (BioTek, Winooski, USA). The reading was subtracted from the reading at 570 nm.

Western blot analysis

Twenty-four hours after irradiation, the medium was removed and washed twice with phosphate-buffered saline (pH 7.4), and the cell lysate was prepared in 200 ml of cold lysis buffer (1 % NP-40, 50 mM Tris–HCl, pH 7.5, 150 mM NaCl, 0.02 % sodium azide, 150 mg/ml PMSF, 2 mg/ml aprotinin, 20 mg/ml leupeptin, and 1 mg/ml pepstatin A). Approximately 30 mg of the cell lysate was separated in a 10 % sodium dodecyl sulfate polyacrylamide gel and transferred onto a polyvinylidene difluoride membrane (Amersham, NJ, USA). The membrane was blocked with a blocking solution containing 5 % skim milk in TBST (2.42 g/l Tris–HCl, 8 g/l NaCl, 0.1 % Tween 20, pH 7.6) for 0.5 h and rinsed briefly in TBST. The membrane was incubated overnight at 4 °C with the appropriate primary antibodies: mouse monoclonal IgG anti-COX-1 (1:1,000, Santa Cruz Biotechnology, CA, USA) and mouse monoclonal IgG anti-COX-2 (1:1,000, Santa Cruz Biotechnology, CA, USA). A mouse monoclonal IgG anti-alpha tubulin antibody (1:2,500, Santa Cruz Biotechnology, CA, USA) was used as the control. Finally, the membrane was washed in TBST, and the immunoreactivity of the proteins was detected using an enhanced chemiluminescence detection kit (Amersham, USA). The levels were determined by densitometric analysis using Scion Image software (Scion Corp, Frederick, MD, USA).

Statistical analysis

All experiments were carried out in triplicate. ANOVA tests were used to evaluate the differences between the sample of interest and its respective control. A P value <0.05 was considered significant.

Results

Determination of LPS concentration

To determine the concentration of LPS that had no effect on cell viability, MC3T3-E1 cells were cultured in a medium containing normal glucose (5 mM) or high glucose (25 mM) for 1 day. A high concentration of mannitol was added to exclude the effect of osmotic pressure on MC3T3-E1 cells. Figure 2 shows the cell viability depending on or according to the LPS concentration. As per the result, the cell viability in each group was increased by 23 and 16 % at low LPS concentrations (0.1 μg/ml) in the normal glucose- and high glucose-containing medium, respectively, whereas it was decreased by 49 and 40 % at high LPS concentrations (100 μg/ml) in the normal glucose- and high glucose-containing medium, respectively. However, 1 μg/ml LPS did not have significant effects on cell viability in the high glucose-containing medium compared to the control, and there were no significant differences between high mannitol and high glucose, which excluded the effect of the osmotic pressure. Therefore, 1 μg/ml LPS was chosen for further study.

Effects of 635 nm LED irradiation on the ROS level

The induction of ROS is controlled by 635 nm irradiation [12]. Flow cytometry showed that DCF fluorescence was enhanced by 9.2 % in the LPS and high glucose-treated group compared to the LPS-treated group. The irradiation groups revealed a 9.1 and 16.4 % decrease in the ROS level in both the LPS alone and LPS with high glucose concentration groups, respectively (Fig. 3a). The microscopic finding showed that the DCF fluorescence obviously vanished in the irradiation groups of LPS with high- and normal glucose-treated groups (Fig. 3b). Therefore, the ROS level in LPS-induced inflammation was enhanced by high glucose levels and was decreased by 635 nm LED irradiation.

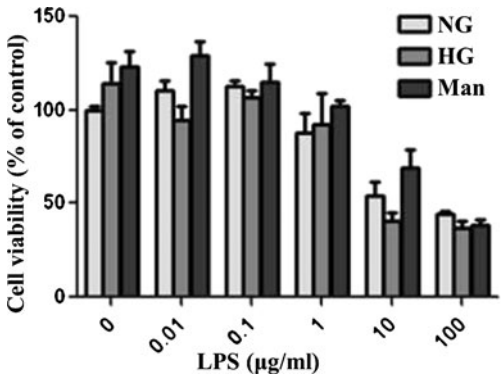

Fig. 2 Effects of LPS concentration and osmotic pressure on the high glucose-induced cell viability. The cell viability was assessed using a MTT assay for the indicated concentrations of LPS (0, 0.01, 0.1, 1, 10, and 100 μg/ml) after 635 nm LED irradiation for 1 h. Data are reported as the mean±SD (n=3)

Effects of 635 nm LED irradiation on inflammation-associated gene and protein expressions

COX induces PGE_2 under inflammatory conditions. The expression of the COX-1 and COX-2 genes was assessed using quantitative real-time PCR at 2, 4, 8, 12, and 24 h (Fig. 4a, b), and the expression of the corresponding proteins was determined using Western blotting at 24 h (Fig. 4c). The expression of the COX-1 gene in the combination of LPS and high glucose level group was higher at 2 and 24 h, compared to the other times. At 2 h, high glucose levels enhanced the LPS-induced gene expression of COX-1 and COX-2 by 20 and 50 %, respectively. Six hundred thirty-five nanometers LED irradiation suppressed the expression of the COX-1 and COX-2 genes in the combination of LPS and high glucose level group by 50 and 33 %, respectively, compared to that in the group without irradiation. After 635 nm LED irradiation, the protein expression of COX-1 and COX-2 at 24 h was also 20 and 51 % lower, respectively, in the combination of LPS and high glucose level group; PGE_2 production was examined by ELISA at 2, 4, 8, 12, and 24 h (Fig. 5). The level of LPS-induced PGE_2 production was higher with high glucose levels than with normal glucose levels at 8, 12, and 24 h. On the other hand, 635 nm LED irradiation of the cells exposed to the combination of LPS and high glucose level inhibited the increase in PGE_2 production at 24 h by 34 % compared to the non-irradiated samples.

Effects of 635 nm LED irradiation on osteoclastogenesis-related gene and protein expressions

Six hundred thirty-five nanometers LED irradiation suppresses the inflammatory pathway inducing PGE_2, which is known as a potent stimulator of osteoclastogenesis. Therefore, the effect of 635 nm LED irradiation on the osteoclastogenesis-related molecules, such as OPG and RANKL, in MC3T3-E1 cells was examined. The gene and protein expressions of RANKL and OPG were affected by the presence of LPS with normal- or high glucose levels in the culture (Figs. 6 and 7). In the presence of LPS with high glucose levels, 64 % of the OPG gene expression was

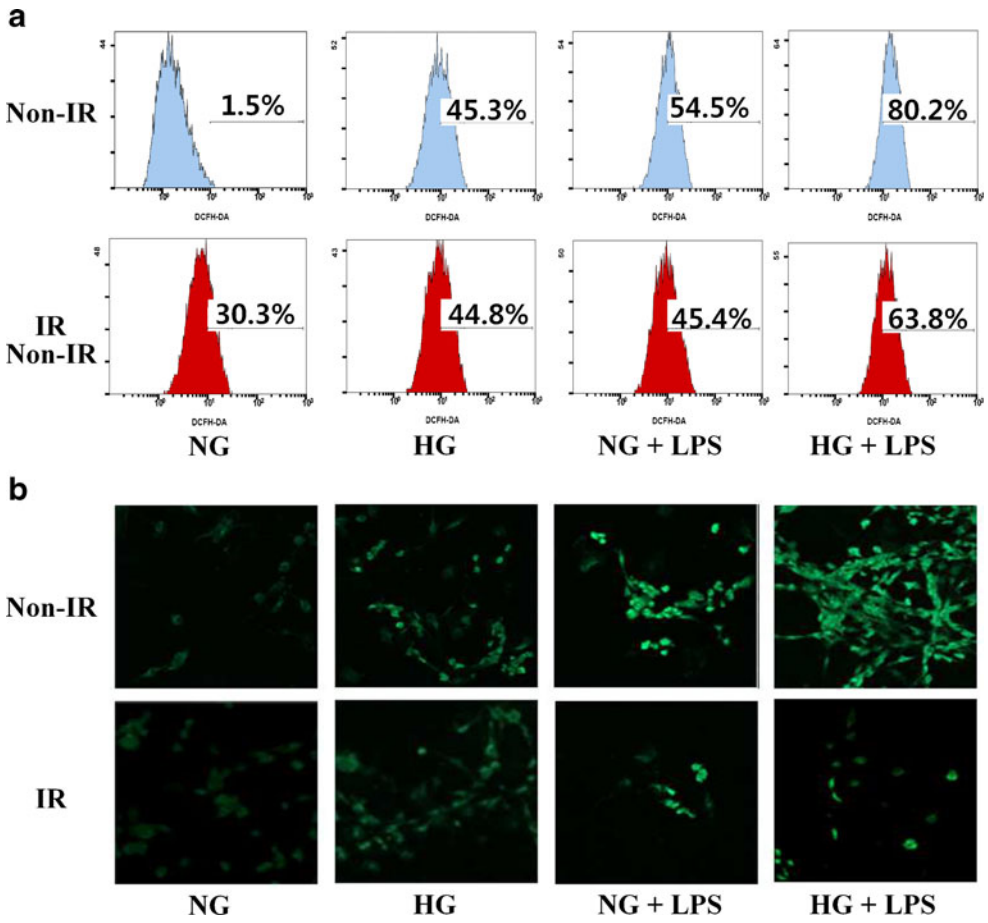

Fig. 3 Effects of 635 nm LED irradiation on ROS formation. **a** Green fluorescence of DCF-DA, indicating intracellular ROS formation, was detected by confocal microscopy. After irradiation, ROS formation was decreased in MC3T3-E1 cells. **b** The DCF fluorescence distribution is represented by flow cytometry histograms (*X-axis* log of the fluorescence intensity from 10^0 to 10^4; *Y-axis* cell number from 0 to 100). Figures are representative of three experiments

blocked and a fourfold increase in the level of RANKL gene expression was observed at 24 h compared to that with normal glucose levels. In the presence of LPS with high glucose levels, 635 nm irradiation resulted in a sixfold increase in the level of OPG gene expression, whereas it decreased the level of the RANKL gene expression by 22 %. The protein expression of RANKL and OPG at 24 h was also affected by 635 nm irradiation. In the presence of LPS with high glucose levels, 635 nm LED irradiation had stimulatory effects on the protein expression of OPG (46 %) and inhibitory effects on the protein expression of RANKL (21 %).

Discussion

Recently, low-level laser therapy has attracted considerable recognition as an effective anti-inflammatory and bone repair tool [15, 16]. He–Ne laser irradiation (632.8 nm) promotes the proliferation and differentiation of human osteoblasts in vitro, and low-power light from a Ga–As–Al laser (830 nm) has a positive effect on osteoblast proliferation [15, 17]. In addition, low-level laser therapy significantly accelerates the wound healing process in experimental diabetic models [18, 19]. However, most studies were related to bone healing and fibroblast proliferation in diabetic patients, whereas the effect of red light irradiation in diabetic periodontitis is still unclear.

The present study examined the effect of 635 nm LED irradiation on the inflammation and osteoclastogenesis-related factors in high glucose-treated osteoblasts in an attempt to model predict its effects in diabetic periodontitis. In the diabetic periodontitis model, 25 mM D-glucose and 1 μg/ml LPS from *P. gingivalis* were applied to MC3T3-E1 osteoblasts. The findings suggest that high glucose enhances the LPS-induced inflammation and 635 nm LED irradiation regulates the inflammatory pathway in MC3T3-E1 osteoblasts effectively. Interestingly, high glucose levels did not have a significant effect and LPS stimulation resulted in a fourfold increase in the expression of the PGE_2, a final inflammatory product. However, the combination of high glucose levels and LPS led to a fivefold stimulation of the PGE_2. Similar glucose-boosted augmentation was observed at the mRNA and protein levels of COX-1 and COX-2. Obviously, there are synergistic inflammatory responses between high glucose levels and LPS. On the

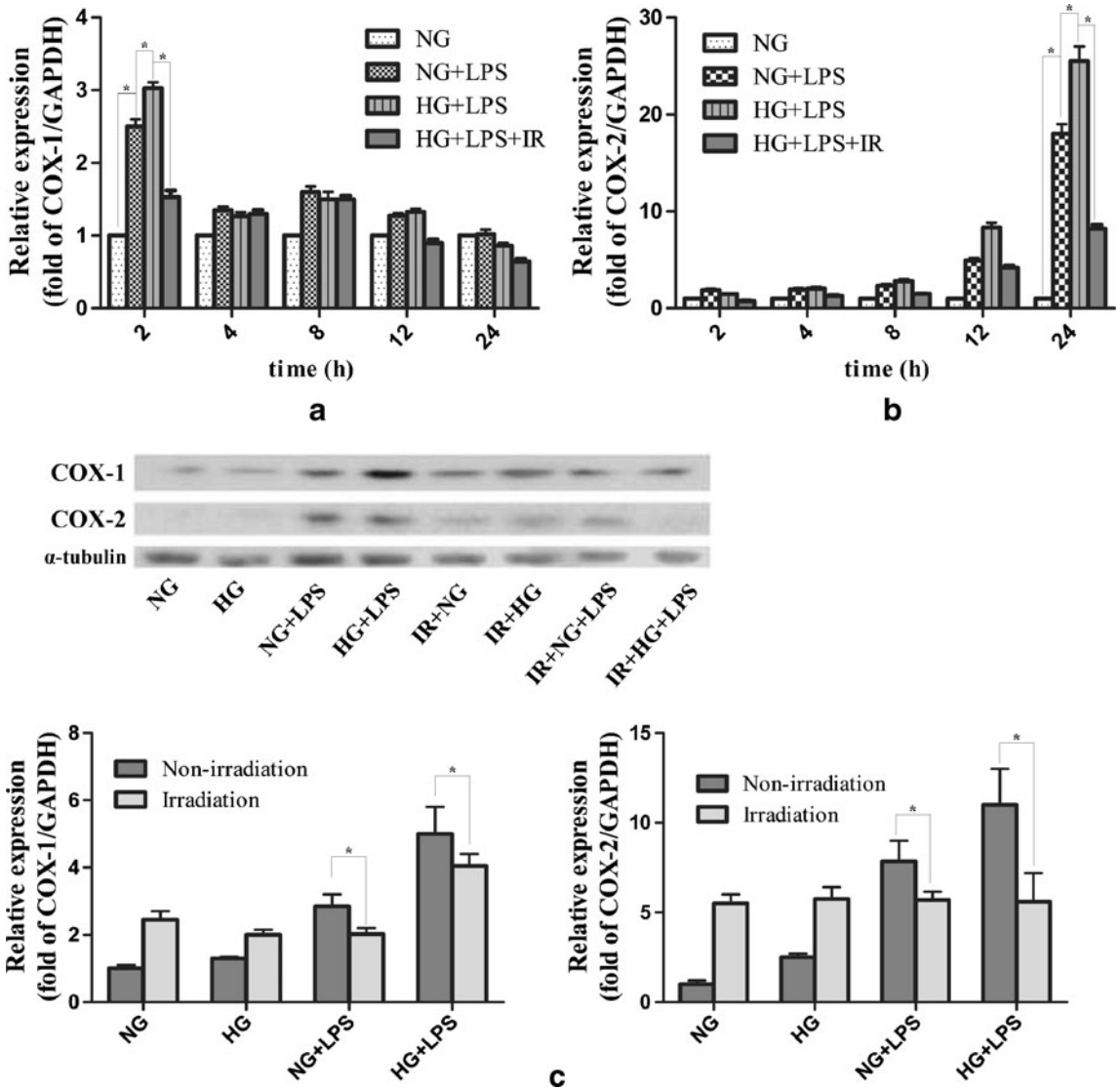

Fig. 4 Effects of 635 nm LED irradiation on COX-1 and COX-2 expression. MC3T3-E1 cells were cultured with or without LPS and high glucose levels for up to 24 h. **a**, **b** COX-1 and COX-2 gene expressions were examined at 2, 4, 6, 8, 12, and 24 h. **c** COX-1 and COX-2 protein expressions were determined at 24 h. The cells were processed for Western blot analysis utilizing GAPDH to ensure equal protein loading. The results were similar in the three separate experiments processed; the mean±SD was obtained by densitometry, as shown in graphic analysis. Significant differences were observed at $*p<0.05$

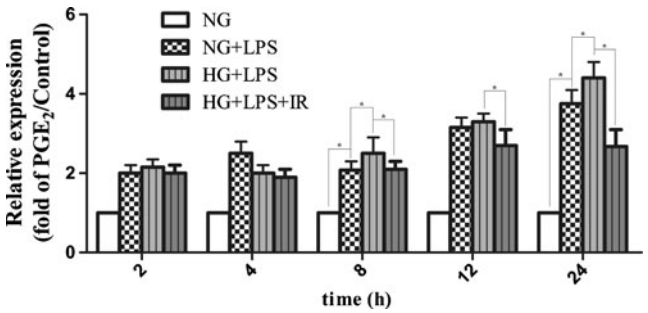

Fig. 5 Effects of 635 nm LED irradiation on PGE_2 production. MC3T3-E1 cells were cultured with or without LPS and high glucose for up to 24 h, and the amount of PGE_2 was determined using ELISA at 2, 4, 6, 8, 12, and 24 h. *Each bar* indicates the mean±SD of three experiments. Significant differences were observed at $*p<0.05$

other hand, the responses of osteoclastogenesis-related molecules to LPS and high glucose levels are more complicated than the inflammatory responses because the effect of high glucose levels on the osteoclastogenesis-related factors is still controversial [20, 21]. In this study, high glucose levels increased the protein expression of OPG and RANKL, and the combination of LPS and LPS high glucose levels decreased the level of OPG protein expression and increased that of RANKL expression. The role of high glucose levels in osteoblasts is still questionable but the results showed that high glucose levels with LPS increase osteoclastogenesis. Therefore, this study has established a good cell model for examining high glucose-boosted inflammation in osteoblasts, which may represent a diabetic

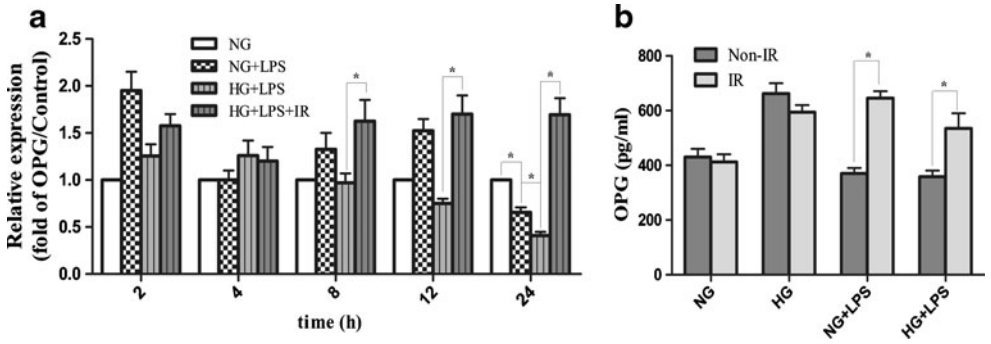

Fig. 6 Effects of 635 nm LED irradiation on the OPG gene and protein expression. MC3T3-E1 cells were cultured with or without LPS and high glucose for up to 24 h. **a** OPG gene expression was examined at 2, 4, 6, 8, 12, and 24 h and **b** OPG protein expression was determined using ELISA at 24 h. Each bar indicates the mean±SD of three experiments. Significant differences were observed at $*p<0.05$

periodontitis model caused by hyperglycemia and bacterial infections.

Previous studies reported that 635 nm LED irradiation has anti-inflammatory effects through the regulation of ROS, which are the critical factors in a range of inflammatory processes through COX inhibitors [12, 22, 23]. In addition, the effect of ROS on osteoblasts has been studied under high glucose conditions [24]. In the present study, the levels of ROS, COX-1, COX-2, and PGE_2 in the LPS-treated cells exposed to normal or high glucose levels were decreased by 635 nm LED irradiation for 1 h. At 24 h, 635 nm LED irradiation of the cells exposed to a combination of LPS and high glucose level reduced the level of PGE_2 production from fivefold to threefold. This shows that 635 nm LED irradiation decreases the level of inflammation, even though high glucose level enhances the inflammatory condition. There are no reports showing that high glucose-boosted inflammation is suppressed by 635 nm LED irradiation, while the anti-inflammatory effect of 635 nm LED irradiation is known.

Furthermore, osteoclastogenesis-related factors are regulated after irradiation. As per this result, the level of OPG expression was increased, whereas the level of RANKL expression was decreased in the diabetic periodontitis model after 635 nm LED irradiation in vitro. Two hypotheses can explain this result. First, 635 nm LED irradiation may directly affect the osteoclastogenesis-related molecules, OPG and RANKL, via ROS regulation. ROS such as H_2O_2 or superoxide anion are involved in bone loss-related diseases by stimulating osteoclast differentiation and bone resorption [25]. However, it is unclear how ROS works in bone metabolism and bone resorption. From this hypothesis, it is believed that 635 nm LED irradiation affects inflammation and bone resorption separately through the regulation of ROS. Second, 635 nm LED irradiation may indirectly affect the osteoclastogenesis-related molecules by regulating inflammation, in which ROS has a pivotal role [26]. The relationship between PGE_2 and periodontal disease has been studied extensively [27, 28]. Klein and Raisz reported that PGE_2 is a potent stimulator of bone resorption [29]. Therefore, 635 nm LED irradiation affects only inflammation, and the inhibition of osteoclastogenesis-related molecules is an additional anti-inflammatory effect of 635 nm LED irradiation. Despite these differences, it is believed that both direct and indirect effects might have a common relationship with ROS.

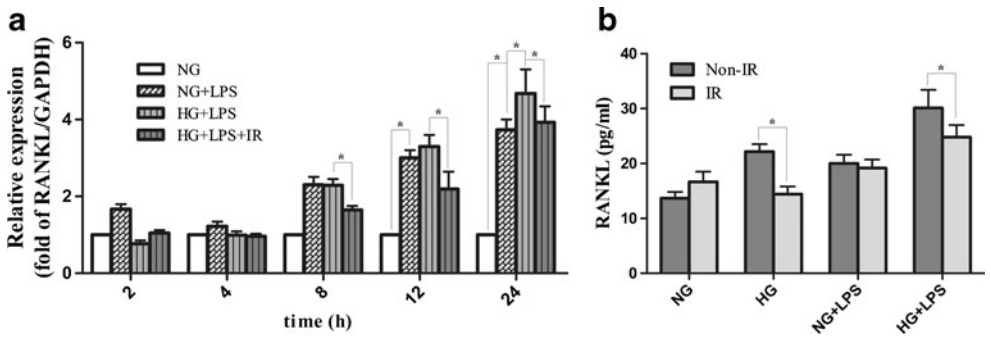

Fig. 7 Effects of 635 nm LED irradiation on the RANKL gene and protein expression. The MC3T3-E1 cells were cultured with or without LPS and high glucose for up to 24 h. **a** RANKL gene expression was examined at 2, 4, 6, 8, 12, and 24 h and **b** RANKL protein expression was determined using ELISA at 24 h. *Each bar* indicates the mean±SD of three experiments. Significant differences were observed at $*p<0.05$

Conclusion

This present study showed that a high glucose level (25 mM) enhances lipopolysaccharide-induced inflammatory factors, such as COX-1, COX-2, and PGE_2, in osteoblasts. In addition, OPG expression was stimulated and RANKL expression was inhibited by 635 nm LED irradiation. Therefore, this study showed that high glucose levels boosted the inflammatory response in MC3T3-E1 osteoblasts, which was reduced by 635 nm LED irradiation. This suggests that 635 nm LED irradiation might be useful not only in reducing inflammation but also in diminishing osteoclastogenesis. Furthermore, 635 nm LED irradiation might be a useful treatment modality for patients with diabetic periodontitis.

Acknowledgments This work was supported by a Korea Research Foundation Grant funded by the Korean Government (MOEHRD) (KRF-2009-0068761).

References

1. Mealey BL, Oates TW (2006) Diabetes mellitus and periodontal diseases. J Periodontol 77:1289–1303
2. Page RC (1991) The role of inflammatory mediators in the pathogenesis of periodontal disease. J Periodontal Res 26:230–242
3. Kannel WB, McGee DL (1979) Diabetes and cardiovascular disease. The Framingham study. JAMA 241:2035–2038
4. Pyorala K, Laakso M, Uusitupa M (1987) Diabetes and atherosclerosis: an epidemiologic view. Diabetes Metab Rev 3:463–524
5. Lalla E, Lamster IB, Feit M, Huang L, Spessot A, Qu W, Kislinger T, Lu Y, Stern DM, Schmidt AM (2000) Blockade of RAGE suppresses periodontitis-associated bone loss in diabetic mice. J Clin Invest 105:1117–1124
6. Lalla E, Lamster IB, Schmidt AM (1998) Enhanced interaction of advanced glycation end products with their cellular receptor RAGE: implications for the pathogenesis of accelerated periodontal disease in diabetes. Ann Periodontol 3:13–19
7. Nair SP, Meghji S, Wilson M, Reddi K, White P, Henderson B (1996) Bacterially induced bone destruction: mechanisms and misconceptions. Infect Immun 64:2371–2380
8. Suda K, Udagawa N, Sato N, Takami M, Itoh K, Woo JT, Takahashi N, Nagai K (2004) Suppression of osteoprotegerin expression by prostaglandin E2 is crucially involved in lipopolysaccharide-induced osteoclast formation. J Immunol 172:2504–2510
9. Tsukii K, Shima N, Mochizuki S, Yamaguchi K, Kinosaki M, Yano K, Shibata O, Udagawa N, Yasuda H, Suda T, Higashio K (1998) Osteoclast differentiation factor mediates an essential signal for bone resorption induced by 1 alpha,25-dihydroxyvitamin D3, prostaglandin E2, or parathyroid hormone in the microenvironment of bone. Biochem Biophys Res Commun 246:337–341
10. Hou JF, Zhang H, Yuan X, Li J, Wei YJ, Hu SS (2008) In vitro effects of low-level laser irradiation for bone marrow mesenchymal stem cells: proliferation, growth factors secretion and myogenic differentiation. Lasers Surg Med 40:726–733
11. Li WT, Leu YC (2007) Effects of low level red-light irradiation on the proliferation of mesenchymal stem cells derived from rat bone marrow. Conf Proc IEEE Eng Med Biol Soc 2007:5830–5833
12. Lim W, Lee S, Kim I, Chung M, Kim M, Lim H, Park J, Kim O, Choi H (2007) The anti-inflammatory mechanism of 635 nm light-emitting-diode irradiation compared with existing COX inhibitors. Lasers Surg Med 39:614–621
13. Lim W, Kim J-H, Gook E, Kim J, Ko Y, Kim I, Kwon H, Lim H, Jung B, Yang K, Choi N, Kim M, Kim S, Choi H, Kim O (2009) Inhibition of mitochondria-dependent apoptosis by 635-nm irradiation in sodium nitroprusside-treated SH-SY5Y cells. Free Radic Biol Med 47:850–857
14. Lim WB, Kim JS, Ko YJ, Kwon H, Kim SW, Min HK, Kim O, Choi HR, Kim OJ (2011) Effects of 635 nm light-emitting diode irradiation on angiogenesis in $CoCl_2$-exposed HUVECs. Lasers Surg Med 43:344–352
15. Garavello-Freitas I, Baranauskas V, Joazeiro PP, Padovani CR, Dal Pai-Silva M, da Cruz-Hofling MA (2003) Low-power laser irradiation improves histomorphometrical parameters and bone matrix organization during tibia wound healing in rats. J Photochem Photobiol B 70:81–89
16. Honmura A, Yanase M, Obata J, Haruki E (1992) Therapeutic effect of Ga–Al–As diode laser irradiation on experimentally induced inflammation in rats. Lasers Surg Med 12:441–449
17. Davis W Jr, Ronai Z, Tew KD (2001) Cellular thiols and reactive oxygen species in drug-induced apoptosis. J Pharmacol Exp Ther 296:1–6
18. Akyol UK, Gungormus M (2010) Effect of biostimulation on healing of bone defects in diabetic rats. Photomed Laser Surg 28:411–416
19. Bayat M, Abdi S, Javadieh F, Mohsenifar Z, Rashid MR (2009) The effects of low-level laser therapy on bone in diabetic and nondiabetic rats. Photomed Laser Surg 27:703–708
20. Balint E, Szabo P, Marshall CF, Sprague SM (2001) Glucose-induced inhibition of in vitro bone mineralization. Bone 28:21–28
21. Secchiero P, Corallini F, Pandolfi A, Consoli A, Candido R, Fabris B, Celeghini C, Capitani S, Zauli G (2006) An increased osteoprotegerin serum release characterizes the early onset of diabetes mellitus and may contribute to endothelial cell dysfunction. Am J Pathol 169:2236–2244
22. Im JY, Kim D, Paik SG, Han PL (2006) Cyclooxygenase-2-dependent neuronal death proceeds via superoxide anion generation. Free Radic Biol Med 41:960–972
23. Murakami M, Kudo I (2004) Recent advances in molecular biology and physiology of the prostaglandin E2-biosynthetic pathway. Prog Lipid Res 43:3–35
24. Wittrant Y, Gorin Y, Woodruff K, Horn D, Abboud HE, Mohan S, Abboud-Werner SL (2008) High d(+)glucose concentration inhibits RANKL-induced osteoclastogenesis. Bone 42:1122–1130
25. Bai XC, Lu D, Liu AL, Zhang ZM, Li XM, Zou ZP, Zeng WS, Cheng BL, Luo SQ (2005) Reactive oxygen species stimulates receptor activator of NF-kappaB ligand expression in osteoblast. J Biol Chem 280:17497–17506
26. Uno K, Nicholls SJ (2010) Biomarkers of inflammation and oxidative stress in atherosclerosis. Biomark Med 4:361–373
27. Goodson JM, Dewhirst FE, Brunetti A (1974) Prostaglandin E2 levels and human periodontal disease. Prostaglandins 6:81–85
28. Offenbacher S, Heasman PA, Collins JG (1993) Modulation of host PGE2 secretion as a determinant of periodontal disease expression. J Periodontol 64:432–444
29. Klein DC, Raisz LG (1970) Prostaglandins: stimulation of bone resorption in tissue culture. Endocrinology 86:1436–1440